

Anti-cancer studies of noble metal nanoparticles synthesized using different plant extracts

Deshpande Raghunandan · Bhat Ravishankar · Ganachari Sharanbasava ·
D. Bedre Mahesh · Vasanth Harsoor · Manjunath S. Yalagatti · M. Bhagawanraju ·
A. Venkataraman

Received: 10 February 2011 / Accepted: 26 April 2011 / Published online: 10 May 2011
© Springer-Verlag 2011

Abstract Biofunctionalized gold and silver nanoparticles synthesized using different plant extracts of guava and clove in vitro anti-cancer efficacy against four different cancer cell lines human colorectal adenocarcinoma, human kidney, human chronic myelogenous, leukemia, bone marrow, and human cervix have been studied and reported. The present experimental study suggests that flavonoids functionalized gold nanoparticles synthesized using aqueous clove buds extract are more potential than guava leaf extract towards anti-cancer activities. The microscopic and 2,3-bis (2-methoxy-4-nitro-5-sulfophenyl)-5-[(phenylamino) carbonyl]-2H-tetrazolium hydroxide (XTT) assay infer that the functionalized irregular shaped gold nanoparticles synthesized with aqueous clove bud extract showed a satisfactory

anti-cancer effect on all the cell lines. The silver nanoparticles synthesized using same extracts are devoid of anti-cancer activity. The XTT assay revealed dose-dependent cytotoxicity to cancer cell lines. The study revealed that the free radicals generated by gold nanoparticles are responsible for anti-cancer effect. To confirm the free-radical scavenging efficacy of gold nanoparticle, nitric oxide assay is followed. We observed that the gold nanoparticles swabbed the free radicals in dose-dependent manner. With continued improvements, these nanoparticles may prove to be potential anti-cancer agents.

Keywords Flavonoid functionalized gold and silver nanoparticles · Cell lines · In vitro activity · XTT assay · Anti-cancer agent

D. Raghunandan
HKES Matoshree Taradevi Rampure
Institute of Pharmaceutical Sciences,
Sedam Road, Gulbarga-585105 Karnataka, India

B. Ravishankar · G. Sharanbasava · D. B. Mahesh ·
A. Venkataraman (✉)
Materials Chemistry Laboratory, Department of Material Science,
Gulbarga University,
Gulbarga 585106, Karnataka, India
e-mail: raman_chem@rediffmail.com

V. Harsoor
Periferal Cancer Institute,
Sedam Road, Gulbarga-585105 Karnataka, India

M. S. Yalagatti
Sri Krupa institute of Pharmaceutical Sciences,
Village Velkatta, Siddipet-502277, Medak, Andhra Pradesh, India

M. Bhagawanraju
CM College of Pharmacy,
Maisammaguda, Dulapally, Hyderabad-500014,
Andhra Pradesh, India

1 Introduction

Cancer is observed as the most dangerous class of disease categorized by uncontrolled cell growth (Chow 2010; Suriamoorthy et al. 2010). There is a marginal increase in cancer cases in the last few years, and most of the time, it ends up with taking life (Dite et al. 2010; Parveen and Sahoo 2010; Smith et al. 2010). In many types of cancer, we are yet to find a satisfactory medicine or carrier of medicine as in case of drug delivery to be used as a satisfactory chemotherapeutic agent. Nanotechnology, an interdisciplinary research field comprising chemistry, engineering, biology, and medicine, has great potential for early detection, accurate diagnosis, and tailored treatment of cancer (Sakamoto et al. 2010). Nanoparticles are usually smaller than several hundred nanometers in size, comparable to large biological molecules such as enzymes, receptors, of a size about 100 to 10,000 times smaller than

human cells. These nanoparticles can offer unprecedented interactions with biomolecules both on the surface and inside the body cells, which may bring revolution in cancer diagnosis and treatment (Seigneuric et al. 2010; Liu et al. 2010).

Nanotechnology is a burgeoning arena which takes along with it a myriad of prospects and possibilities for advancing disease treatment in pharmaceutical and medical field. At nanometric scale, the physico-chemical and biological properties of materials differ fundamentally from their corresponding bulk counterpart because of the size-dependent quantum effect. The noble metal nanoparticles like gold nanoparticles (AuNP), especially surface functionalized represent smart and promising candidates in the drug delivery applications due to their unique dimensions, tunable functionalities on the surface, and controlled drug release (Datar and Richard 2010). Another essential aspect while working with AuNP in bio-applications is safety and biocompatibility (AuNP is already approved by the US Food and Drug Administration.) Biologically synthesized and functionalized, AuNP provide many desirable attributes for use as carriers in drug delivery systems as the functionalized AuNP core is essentially inert and nontoxic 1 reported in recent studies (Han et al. 2007; Kim et al. 2009). Monodispersed nanoparticles can be formed with a core size from <30 nm and also with metal–core–organic–shell morphology; the mono-metal layer can be tailored with a range of biological ligands, help in effective cellular uptake, controlled drug release, and targeted drug delivery (Ghosha et al. 2008; Salmaso et al. 2010). These functionalized nanodelivery systems can be used directly as promising lead molecules in the detection of cancer cells. In this applied research work, we have deduced and detailed the use of synthesized bio-functional noble metal nanoparticles application as an anti-cancer drug and demonstrate the anti-cancer effect of these functionalized AuNP using nitric oxide method. It gives a strong speculation, for the influence of free electrons generated by the surface of the functionalized AuNP has a lethal effect on the electronegative surface membrane of the cancer cells. The free-radical scavenging effect of AuNP is compared with the well-known anti-oxidant butyl hydroxy anisole (BHA), which is determined by nitric oxide method. The end results confirm that functionalizing AuNP with the water-soluble organic moieties can show the synergic anti-proliferative effect in various cancer cell lines, and thus prove to be useful in various types of anti-cancer control systems.

We have already worked for the synthesis of different functionalized Au and Ag nanoparticles using different plant extracts of clove and guava (Raghunandan et al. 2009; Raghunandan et al. 2010a; Raghunandan et al. 2010b). The characterization is elaborately discussed with respect to size, shape stability, and functionalization using different spectroscopic and microscopic techniques. The shape of

silver nanoparticles (AgNP) found to be roughly spherical and in 30–60 nm and 20–30 nm range in case of guava leaf and clove buds-mediated synthesis, respectively. The clove-mediated AuNP yielded highly unpredictable irregular-shaped particles in the range of 5–100 nm, whereas guava leaf-mediated synthesis produced poly-shaped nanoparticles in the narrow range of 25–30 nm. In all the cases of noble nanoparticle synthesis, the preliminary studies using FTIR (Fourier transformed infrared spectroscopy) confirms that the different polyphenols of the flavonoids of the respective plants are responsible for the biosynthesis, and the same are capped on the surface of the nanoparticles. Though the further studies on the exact chemical moiety responsible for bioreduction pathway is still underway, in this paper, we are making an effort to understand the anti-proliferative effect of these functionalized “lead” in different cancer cell lines. The encouraging results of functionalized AuNP as an anti-cancer agent using different plant extract has a promising lead for further exploitation.

2 Experimental

2.1 Biosynthesis of nanoparticles

The AuNP and AgNP were synthesized separately treating the 10^{-3} N HAuCl₄ and 10^{-3} AgNO₃ solutions with guava leaf (*Psidium guajava*) extract and clove bud (*Syzygium aromaticum*) extract, respectively, as reported in our earlier research papers (Raghunandan et al. 2009; Raghunandan et al. 2010a; Raghunandan et al. 2010b) The flavonoid-conjugated AuNP using guava and clove are represented as AuNP-Gua and AuNP-Clo, respectively, and is shown in Fig. 1.

2.2 Anti-cancer activity study

Four different cells lines namely HT-29 (human colorectal adenocarcinoma), HEK-293 (human kidney), K-562 (human chronic myelogenous, leukemia, bone marrow), and HeLa (human cervix) cell lines were obtained from the American Type Culture Collection, USA. The growth media: RPMI-1640, sufficient minimum essential medium (MEM), and the phosphate buffer solution (PBS) tablets were obtained from Sigma Chemical Co., St Louis, USA. Standard quality fetal calf serum, penicillin–streptomycin, and trypsin were obtained from Sigma labs. The XTT kit, which consists of the 2,3-bis(2-methoxy-4-nitro-5-sulfophenyl)-5-[(phenylamino)carbonyl]-2H-tetrazolium hydroxide (XTT) labeling reagent and the solubilisation solution was procured from Sigma labs, USA. Trypsin (0.25%+EDTA, 1 mM in PBSA), XTT dye–50 mg/mL, sterilized Sorensen's glycine buffer (0.1 M glycine, 0.1 M NaCl adjusted to pH 10.5 with 1 M NaOH), DMSO, growth medium is procured from Aldrich

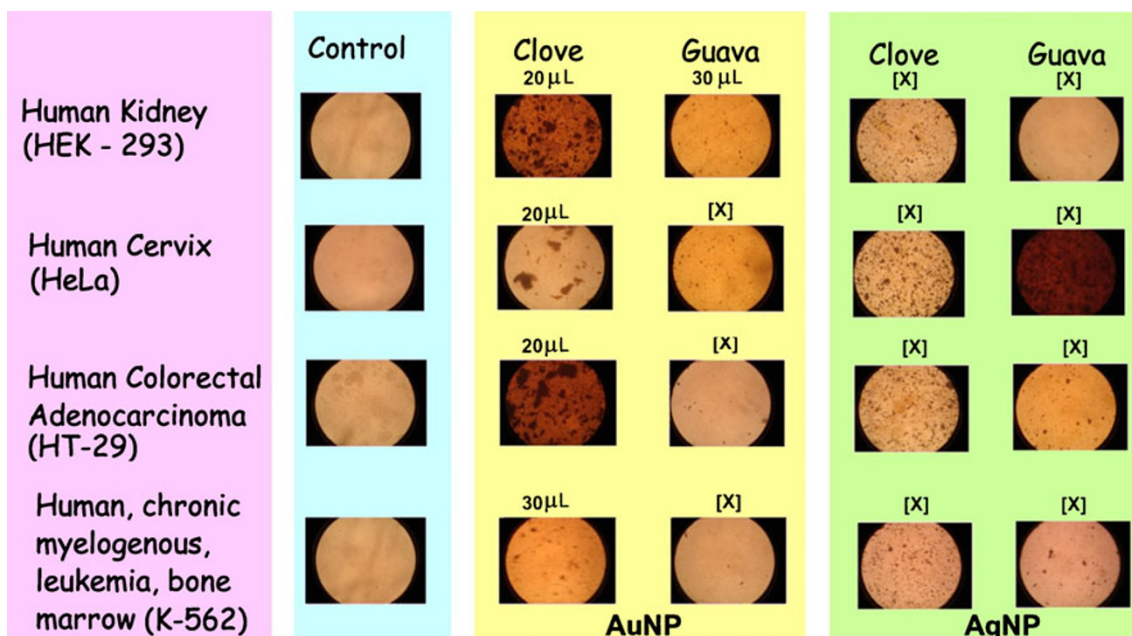


Fig. 1 Microscopic image showing the anti-proliferative effect of AuNP and AgNP synthesized using aqueous extracts of guava leaf and buds of the clove, respectively, at different concentrations. [X] indicates the absence of the activity

labs. XTT labeling reagent and electron-coupling reagent were thawed, respectively, in a water bath at 37°C. Each vial was mixed thoroughly to obtain a clear solution. To perform a cell proliferation assay (XTT) with one microplate (96 wells), 5 mL XTT labeling reagent was mixed with 0.1 mL electron-coupling reagent.

2.3 Free-radical scavenging activity of AuNP

Aqueous solution of AuNP–clo of different concentrations (2.5 µg, 5 µg, 10 µg/µL) were taken in different test tubes and made up to 3 ml with 0.1 M phosphate buffer (pH 7.2). Sodium nitroprusside (5 mM) prepared in buffered saline (pH 7.2) and 1 mL was added to each tube. The reaction mixture was incubated for 30 min at RT. A control without the test compound, but with an equivalent amount of methanol was prepared for comparison purpose. After 30 min, 1.5 mL of above solution was mixed with 1.5 mL of Griess reagent (1% sulphanilamide, 2% phosphoric acid and 0.1% N-1-naphthylethylenediamine dihydrochloride). The absorbance of the samples was measured at 546 nm. Nitric oxide radical scavenging activity was calculated using the following formula:

$$\% \text{ radical scavenging activity} = \left[\frac{(\text{control OD} - \text{aq. AuNP OD})}{\text{control OD}} \right] \times 100$$

2.4 Cell culture

A 96-well micrometer plate equipment (Nunc, Denmark) is used for this experiment. Two hundred microliters of

MEM is added in the required amount of wells; in each cell, 50 µL of different cell lines are added. Biofunctionalized AgNP and AuNP of different concentrations (10, 20, 30 µg/L) were added into the wells separately. The cells were cultured in the appropriate medium supplemented with 5–10% fetal calf serum and 1% penicillin–streptomycin, using 25 cm² flasks in a 37°C incubator with 5% CO₂. To subculture the cells, the cells were separated, and the fresh culture medium was used with fresh medium as follows: in the first step, the old medium was removed, and then the cells were rinsed briefly with PBS. After adding 1–2 µL of trypsin, the flask was incubated at 37°C using 5% CO₂ for 5 min. The upper part of the liquid is discarded, and the detached cells, which are present in the lower part of the flask, are taken in another flask, and after adding 20 µL of medium to it, the culture was divided in two parts. One part was then transferred to a new flask. The cells were grown till they become turbid and confluent. Then, trypsin is added to these cells to prepare a cell suspension, and the numbers of viable cells were counted with a hemocytometer. One hundred microliters of suspension containing 1 × 10⁵ cells was seeded in each well of a 96-well microtiter plate. The plate was then incubated overnight at 37°C with 5% CO₂. Periodically, the medium was replaced.

2.5 Cell proliferation assay

Each cancer cell line was grown in a 96-well microtiter plate of a final volume of 100 µL culture medium per well. The cells were then treated with functionalized AgNP and AuNP developed with different plant extract and bio-

excretories at a dose of 10, 20, and 30 $\mu\text{g}/\text{mL}$ and maintained them in incubator at 37°C with CO_2 for 48 h. Fifty microliters of the saturating solution (Roche Diagnostics, USA) was then added into each well. The plate was kept overnight in the incubator. Viability of the cells was counted using an ELISA reader (ELx 800) at 550 nm. The experiment was carried out in six replicates.

2.6 Measurement of growth-inhibitory effect

Cells were grown in 96-well plates in a final volume of 100 μL of culture medium per well. Each well contained 1×10^5 cells/mL and was incubated for 24 h in a 5% CO_2 incubator at 37°C . As detailed above, the same procedure was adopted for cell culture. The HeLa cell line was used as it has the lowest IC_{50} (the concentration of test compound that can inhibit 50% of the cancer cells from proliferating) for functionalized AuNP and the same was observed using microscope. The cells were treated with different nanoparticles at a concentration that was similar to the IC_{50} value. The plate was then incubated again in the 5% CO_2 incubator at 37°C for 48 h. The untreated cells (control) were also incubated for 48 h. The growth of the cells was photographed using a phase contrast microscope (Olympus, USA). Cells, grown in a 96-well tissue culture plate, are incubated with the yellow XTT solution (0.3 mg/mL) for additional 4 h.

The cells were grown till they become turbid and confluent. Trypsin is then added to the cells to prepare a cell suspension, and the number of viable cells was counted with a hemocytometer. Fifty microliters of suspension containing 1×10^5 cells was seeded in each well of a 96-well microtiter plate. The plate was then incubated overnight at 37°C with 5% CO_2 . Periodically, the medium was replaced. A 96-well micrometer plates are used for this experiment. Two hundred microliters of MEM is added in the required number of wells; to this, 50 μL of different cell lines are added in each well. Biofunctionalized AuNP of different concentrations (10, 20, 30 μL) were administered into the wells separately. The cells were cultured in the appropriate medium, supplemented with 5–10% fetal calf serum and 1% penicillin–streptomycin, using 25 cm^2 flasks in a 37°C incubator with 5% CO_2 . To subculture the cells, the cells were separated, and the fresh culture medium was used with fresh medium as follows: in the first step, the old medium was removed, and then the cells were rinsed briefly with PBS to wash the cells. After this, 1–2 μL of trypsin was added, and the flask was incubated at 37°C and 5% CO_2 for 5 min. The upper part of the liquid is discarded, and the remaining detached cells, present in the lower part of the flask, are taken in a separate flask; 20 μL of medium was added, and the culture was divided in two parts. One part of this was transferred to a new flask.

3 Result and discussion

Functionalized AuNP developed with clove buds extract (AuNP-Clo) inhibit 50% of the proliferation of HeLa, HEK-293, and HT-29 cancer cells at 20 $\mu\text{g}/\text{mL}$ concentration. The same nanoparticles inhibited the K-562 cancer cell line at 30 $\mu\text{g}/\text{mL}$ concentration. This colorimetric assay is based on the capacity of mitochondria succinate dehydrogenase enzymes in living cells to reduce the yellow water-soluble substrate XTT into an insoluble, colored formazan product, and therefore, this conversion only occurs in viable cells (Berridge et al. 1996). Additional incubation period for 4 h after the addition of XTT labeling reagent, the change in the color of the solution in different wells is observed. A solution of orange formazan is formed, which is quantified spectrophotometrically using an ELISA plate reader at 490 nm (Sacconi et al. 2009). For this, a graph of absorbance against drug (AuNP) concentration was plotted and the inhibitory effect (IC_{50}) was calculated. The reduction of XTT can only occur in metabolically active cells; the level of activity is a measure of viability of cells. Absorbance values that are lower than the control cell lines reveals decline in the rate of cell proliferation. Conversely, a higher absorbance indicates an increase in the cell proliferation. Untreated microtiter plates of cell lines with only vehicle (0.3% v/v DMSO in water) is considered as proliferative control.

An increase in number of living viable cells results in an increase in the total activity of mitochondrial dehydrogenases in the anti-malignant cells. As observed by the absorbance, the increase is directly proportional to the orange formazan formed quantitatively, (Leviar et al. 2003). This process is safe, unlike available other alternatives, as no radioactive isotopes are used. The results found are precise and can be correlated to the number of viable cell number. The method is also sensitive and can be used for large number of samples. The inhibition of cell proliferation percentage by the AuNP with different plant extracts was calculated based on difference in inhibitory effect between treated cell lines and their respective controls, where 100% cell proliferation was taken from corresponding controls. Table 1 shows growth of inhibitory effect of functionalized AuNP on different cell lines. From the table, it is evident that clove flavonoids-conjugated AuNP can be used effectively at a very low concentration against different types of cancer.

3.1 Statistical analysis

All the results are expressed as mean \pm SD of triplicate. The difference in inhibitory effect at different doses between treated and corresponding controls was analyzed for statistical significance by performing Student's *t* test. $P < 0.05$ implies significance. Nil inhibitory effect on

Table 1 Growth-inhibitory effect of functionalized AuNP on different cell lines

Treatment	Inhibitory effect on cell lines (IC ₅₀)				
	HEK-293	HeLa	HT-29	HEK-293	Vero
AuNP-Clo	19.88±0.006* (62.89%)	20.05±0.002* (58.77%)	20.12±0.007* (56.78%)	28.56±0.010** (51.55%)	56.78±0.001 (32.56%)
AuNP-Gua	31.22±0.011 (48.56%)	36.11±0.001 (42.45%)	39.44±0.010 (38.54%)	45.67±0.002 (35.66%)	61.23±0.005 (28.44%)

Each value represents mean±SD. Data were analyzed by Student's *t* test. Number in the *parenthesis* denotes percent inhibition of cell proliferation **P*<0.01, ***P*<0.05 vs. corresponding control

cancer cell lines was observed by both extracts at dilutions less than 10 µg/mL. Anti-proliferative activity of ethanol extract on Vero cell line was constantly less at experimented dilutions as compared to cancer cell lines.

3.2 Growth-inhibitory effect

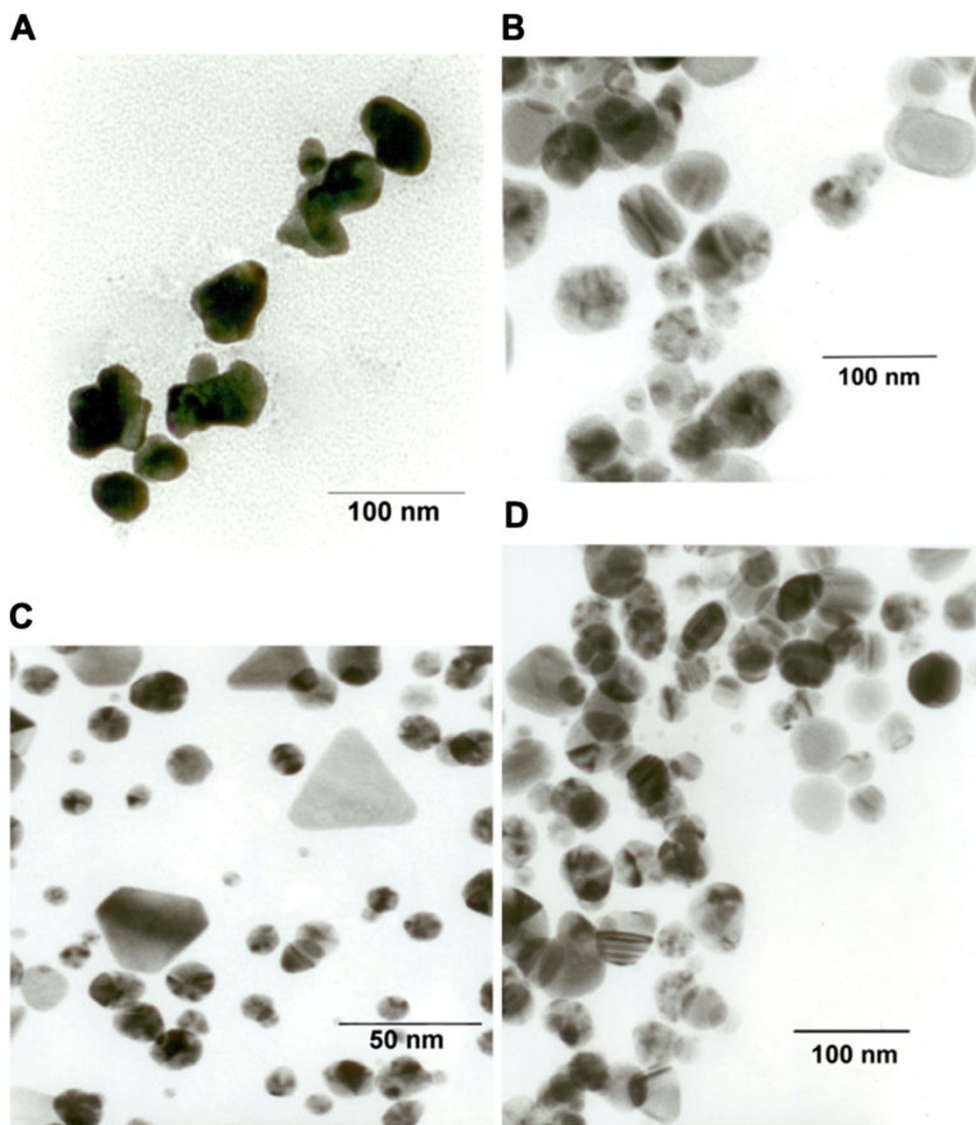
The ability of AuNP developed from clove extract inhibit proliferation of HEK-293, HeLa, and HT-29 cell line at 20 µg/mL was estimated by its observed effect on the growth of the cells. The growth of the untreated (control) and treated HEK-293, HeLa, and HT-29 cell line after incubation for 48 h was photographed using a phase-contrast microscope. The observation of HEK-293, HeLa, and HT-29 cells showed that most of the cells were attached in the culture containing 20 µg/mL of AuNP functionalized with clove moieties. The cells were viable and adhered to the bottom of the well after 48 h of treatment, although a large proportion of the cells were found in isolated condition. Cells of all cancer cell lines are shrunken and isolated condition after 48 h of incubation. The effect of functionalized gold and AgNP on the proliferation of human cancer cells was determined. The percentage of cell viability was measured by comparing the optical density (OD) of abovementioned cancer cells culture treated with different functionalized AuNP against the control. AuNP synthesized from clove, causes 50% cell death in all human cancer cell lines tested. In this study, clove extract-mediated AuNP has been proven to inhibit the proliferation of three cancer cell lines out of four that were tested at a strong IC₅₀ value (<20 µg/mL). These nanoparticles was not active (IC₅₀>30 µg/mL) against K-562. Figure 2 shows the microscopic images of wells containing the different cancer cell lines treated with different flavonoid-conjugated AuNP and AgNP. The XTT assay as discussed above is done on only flavonoid-conjugated AuNP based on the positive results obtained by this microscopic analysis.

The freely water-soluble flavonoids present in the guava leaf and clove buds solution that could have been adsorbed on the surface can stimulate or suppress the immune system

due to the presence of –OH groups. Presence of such phenolic moieties may be assumed to have synergic effect for the anti-proliferative activities of these bio-adsorbed metal nanoparticles (Kawai et al. 1999; Salucci et al. 2002; Lee and park 2010). The anti-proliferative activity is also attributed to the irregular shape of the nanoparticles (Chen et al. 2008). These shape-dependent properties of AuNP have different behaviors and make them suitable for therapeutic utilization (Greenfield 2005; Gobin et al. 2007; Kevin 2008; Sperling et al. 2008; Bertussi et al. 2005). AuNP of certain non-regular shapes can readily be adsorbed to the surfaces of the biomolecules which show higher surface plasmon resonance and will have a greater contrast effect than those of photothermal dyes that are used regularly in detection of cancer cells (Giljohann et al. 2010; Katti et al. 2006). Here, the bio-detection sensitivity and biocompatibility parameters become very important. The bio-detection sensitivity of nanoparticles often is associated with their physical and chemical properties, which in turn depend on the shape of the particles (Rinaldo et al. 2006; Hu et al. 2007). Nanoparticles with different dimensions have been applied widely to detect biological molecules. Colloidal AuNP is used to detect specific DNA sequences and single-base mutations in a homogeneous format. AuNP synthesized with biological base are interesting, predominantly because they exhibit the best compatibility with biomolecules. But, bio-detection sensitivity derived from spherical nanoparticles is not strong enough to trace the interaction of biomolecules (Maxwell et al. 2002; Orendorff et al. 2006). Looking into all these aspects, it is reasonable to infer that the biosynthesis of irregular-shaped nanoparticles hopefully might reach this aim because they display novel properties and may improve biological detection sensitivity greatly. The shape of the noble nanoparticle will also play important role as an anti-cancer agent. On the basis of our results, we can speculate on the mechanisms that govern shape-dependent extracellular effect of nanoparticles.

The microscopic image in Fig. 2 shows that the same flavonoid-conjugated AgNP are devoid of anti-cancer effect on all the cell lines. This study infers that the flavonoid functionalization helps for reducing the toxicity in the host

Fig. 2 TEM images of AuNP and AgNP synthesized using aqueous extracts of guava leaf and buds of the clove, respectively (reproduced with permission from A) Elsevier, B) & C) Springer)



and offers only synergic effect in case of the functionalized AuNP. The activity might be because of the size, shape, or other intrinsic properties of the gold nanoparticles. Many studies prove that the gold nanoparticles of 30–50 nm range show good anti-cancer effect. At this range, our research shows that the irregular-shaped AuNP offers maximum anti-cancer effect on all the cell line compared to poly-shaped, nearly spherical, or spherical noble nanoparticles. The most possible reason that because of their unpredictable shape, the moment in between the cells, and also the non-specific adsorption to the cell surface is high compared to particles of other shapes. Since these flavonoids are important in the internal stabilization of gold nanoparticles, a further detailed study is needed. This will provide a better understanding of how this flavonoid-conjugated AuNP disturbs and destroys the cell externally. Figure 3 shows the pictorial representation of shape-dependent anti-cancer effect of gold nanoparticles. The irregularly shaped nano-

particles can move easily in between the abnormally high and irregularly spread neoplastic cells compared to poly-shaped or roughly spherical ones; it is reasonable to infer that these special unpredictable amoebic shaped is having better anti-proliferative effect.

As such, the clove extract itself has reported anti-malignant effect at higher concentration in different types of cancer. The morphology of HeLa, HEK-293, and HT-29 cell line that were treated with AuNP-Clo at 20 $\mu\text{g}/\text{mL}$ was

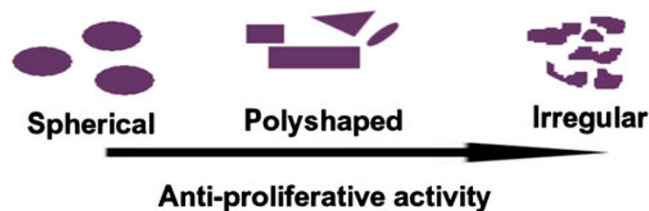
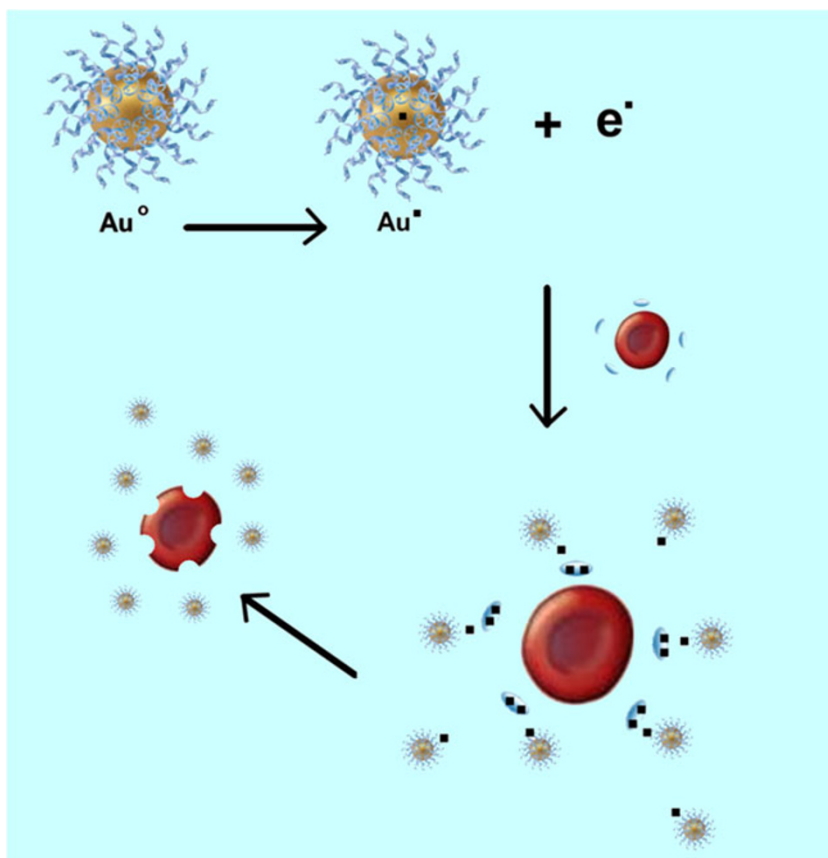


Fig. 3 Shape-dependent anti-proliferative activity of AuNP

Fig. 4 Probable anti-proliferative mechanism of AuNP



studied to prove the effect of these AuNP on the cell growth. Our observations showed that the growth of the cells was inhibited. However, further study is needed to understand the exact mechanism of anti-cancer activity of these nanoparticles. AuNP-Clo proved to possess anti-proliferative properties against all the cancer cell lines tested. The prominent anti-proliferative effect of functionalized AuNP on HEK-293, HeLa, and HT-29 cancer cell lines, as revealed by its IC_{50} based on XTT assay was found to be 19.88 ± 0.006 , 20.05 ± 0.002 , 20.12 ± 0.007 , and 28.56 ± 0.010 , respectively. IC_{50} of AuNP-Clo was specifically less significant on Vero cell line, i.e., 55.3 ± 2.74 . Therefore, it can be said that AuNP-Clo is a promising anti-cancer “lead”. However, the exact mechanism behind the anti-proliferative effects of AuNP-Clo needs to be studied to determine whether the effect is due to an increase in apoptosis. The plasma membrane of the cancer cell defines the separation between the internal constituents of a cell and the outside environment. This semi-permeable membrane allows free diffusion of small and non-polar molecules. However, bigger ones like nanomaterials are incapable of crossing the plasma membrane which requires uptake mechanisms such as endocytosis. Most of bio-functionalized AuNP are easily taken up by the cells through endocytotic mechanisms, but they remain in endosome vesicles, become incapable of reaching the cytosol system. Although endocytotic uptake is

the normal phenomenon for a variety of nanomaterials, the efficiency predominantly depends on shape, size, the dispersivity, and the other physico-chemical parameters. This is important, because there may be many factors that affect the anti-proliferative activity in the in vivo study. Further study is underway.

AuNP-Gua has shown activity against HEK-293 but the $IC_{50} > 30 \mu\text{g/mL}$. These are devoid of anti-proliferative activity against other three cell lines. AuNP developed with cow urine as a reducing agent has shown activity against HeLa, HEK-293, and HT-29 at $30 \mu\text{g/mL}$. Though the

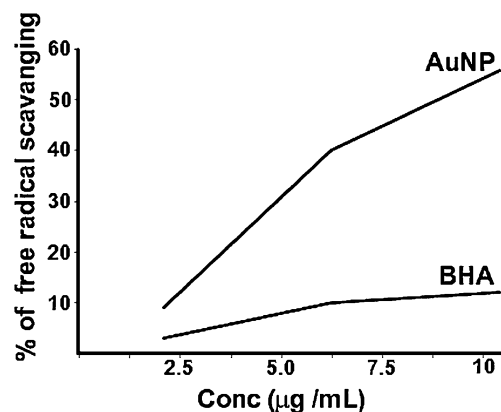


Fig. 5 Graph showing free-radical scavenging activity of AuNP

inhibitory effect is higher than that of AuNP-Clo, but looking in to the beneficial effects of cow urine, the AuNP synthesized with using cow urine as a reducing medium can be a promising anti-cancer agent. Poly-shaped nanoparticles synthesized using guava extract has shown cytotoxic effect on HEK-293 and the IC₅₀. Functionalized AgNP using other different plant extract and bio-excretory have not shown any cytotoxic effect even at 30 µg/mL. This also proves that the adsorbed bio-moieties alone are devoid of cytotoxic effect at that concentration.

To determine the relationship between free-radical and anti-cancer activity, we used nitric oxide method to test whether the antioxidant property could influence anti-cancer activity induced by AuNP. Recently, efficacy of free-radical generation of AuNP is studied and reported using EPR spectroscopy and spin-trapping technique (Ionita et al. 2007). We understand that the anti-cancer effect of AuNP is related to the generation of free radicals and subsequent free radical-induced cancer cell surface damage (Nie et al. 2007). These free radicals attack the nearest neoplastic cell and steals its electron. When the cell loses its electron, it becomes a free radical itself, and begins a chain reaction. When this cascade of reaction is initiated in the surface of the cell wall, within a short time, the total disruption of a living cell is seen. The progression will go on from cell-to-cell which contributes to the electron propagation all around entire part of the tissue. This, in turn, is responsible for shrinkage and rupture of the cell surface and improper nutrient and signal supply. Figure 4 shows the pictorial diagram AuNP lethal effect by generating the free radicals on the cell surface. To confirm the production of free radical, we analyzed the AuNP by nitric oxide method. Figure 5 shows a very encouraging trend in scavenging the NO-free radical in a concentration dependent manner. It could be seen from this figure that AuNP scavenged the NO-free radical five times more effectively than BHA (butylated hydroxyanisole). At concentrations as low as 5 µg, even where BHA had less than 10% efficiency, bio-functionalized AgNP mopped up more than 40% free radical in vitro. Similarly, the percentage of quenching effect on NO-free radical was 9% with AuNP at a minimum concentration of 2.5 µg, where BHA shows only 3% at same concentration. AuNP and BHA scavenged 56% and 12%, respectively, at a maximum concentration of 10 µg. Statistical analysis (test of significance) of the data obtained from the free-radical scavenging activity of AgNP using *t*-test indicated that the difference on the NO-free radical used was significant ($P < 0.01$) than BHA.

4 Conclusion

The development of functionalized targeted gold nanoparticles as therapeutic agents has generated great interest

in both academy and industry. Targeted gold nanoparticles have shown promising results in in vitro studies, signifying that they are potential as therapeutic carriers. This exploration creates the new avenue to a new standard where the different flavonoids-functionalized gold nanoparticles can be a powerful weapon against cancer.

Acknowledgments Financial supports from BRNS (Grant no. 2009/34/14/BRNS) UGC (D.O.No. F.14-4/2001 (Innov. Policy/ASIST)) are acknowledged. We acknowledge SAIF, IIT Mumbai for TEM and Biogenics. Raghunandan Deshpande thank his father Jagannathrao M. Deshpande for editing and Dr. Appala Raju, principal of H.K.E.S's Matoshree Taradevi Rampure Institute of Pharmaceutical Sciences, Gulbarga for encouraging the research program.

References

- Berridge MV, Tan AS, Mccoy KD, Wang R (1996) The biochemical and cellular basis of cell proliferation assays that use tetrazolium salts. *Biochemica* 4:14–19
- Bertussi B, Natoli JY, Commandre M, Rullier JL, Bonneau F, Combis P, Bouchut P (2005) Photothermal investigation of the laser-induced modification of a single gold nano-particle in a silica film. *Opt Commun* 254(4–6):299–309. doi:10.1016/j.optcom.2005.06.004
- Chen PC, Mwakwari SC, Oyeler AK (2008) Gold nanoparticles: From nanomedicine to nanosensing. *Nanotechnol Sci Appl* 537(1):45–66
- Chow AY (2010) Cell cycle control by oncogenes and tumor suppressors: driving the transformation of normal cells into cancerous cells. *Nat Educ* 3(9):7
- Datar RH, Richard JC (2010) Nanomedicine: concepts, status and the future. *Medical Innovation & Business*: 2(3):6–17. doi:10.1097/MNB.0b013e3181ef18fe
- Dite GS, Whitemore AS, Knight JA, John EM, Milne RL, Andrulis IL, Southey MC, McCredie MRE, Giles GG, Miron A, Phipps AI, West DW, Hopper JL (2010) Increased cancer risks for relatives of very early-onset breast cancer cases with and without BRCA1 and BRCA2 mutations. *Br J Canc* 103:1103–1108. doi:10.1038/sj.bjc.6605876
- Ghosha P, Hana G, Dea M, Kima CK, Rotello VM (2008) Gold nanoparticles in delivery applications. *Adv Drug Deliv Rev* 60(11):1307–1315. doi:10.1016/j.addr.2008.03.016
- Giljohann DA, Seferos DS, Daniel WL, Massich MD, Patel PC, Mirkin CA (2010) Gold nanoparticles for biology and medicine. *Nanotechnology, Science and Applications* 49(19):3280–3294. doi:10.1002/anie.200904359
- Gobin MA, Lee MH, Naomi JH, William DJ, Rebekah AD, Jennifer LW (2007) Near-infrared resonant nanoshells for combined optical imaging and photothermal cancer therapy. *Nano Lett* 7:1929–1934. doi:10.1021/nl070610y
- Greenfield SA (2005) Biotechnology, the brain and the future. *Trends Biotechnol* 23(1):34–41. doi:10.1016/j.tibtech.2004.11.011
- Han G, Ghosh P, Rotello VM (2007) Special focus: advances in nanomedicine symposium—review. Functionalized gold nanoparticles for drug delivery. *Nanomedicine* 2(1):113–123. doi:10.2217/17435889.2.1.113
- Hu J, Wang Z, Li J (2007) Gold nanoparticles with special shapes: controlled synthesis, surface-enhanced raman scattering, and the application in bio-detection. *Sensors* 7:3299–3311. doi:10.3390/s7123299

- Ionita P, Conte M, Gilbert BC, Chechik V (2007) Gold nanoparticle-initiated free radical oxidations and halogen abstractions. *Org Biomol Chem* 5:3504. doi:10.1039/B711573C
- Katti KV et al (2006) Nanocompatible chemistry toward fabrication of target-specific gold nanoparticles. *J Am Chem Soc* 128:11342–11343. doi:10.1021/ja063280c
- Kawaii S, Tomono Y, Katase E, Ogawa K, Yano M (1999) Antiproliferative activity of flavonoids on several cancer cell lines. *Biosci Biotechnol Biochem* 63(5):896–899. doi:10.1271/bbb.63.896
- Kevin B (2008) Shape matters for nanoparticles, technology published by MIT review.
- Kim C, Ghosh P, Rotello VM (2009) Multimodal drug delivery using gold nanoparticles. *Nanoscale* 1:61–67. doi:10.1039/b9nr00112c
- Lee S, Park H (2010) Anticancer activity of guava (*Psidium guajava* L.) branch extracts against HT-29 human colon cancer cells. *Journal of Medicinal Plants Research* 4(10):891–896
- Leviar N, Dewey RA, Daley E, Bates TE, Davies D, Kos J, Pilkington GJ, Lah TT (2003) Selective suppression of cathepsin L by antisense cDNA impairs human brain tumor cell invasion in vitro and promotes apoptosis. *Canc Gene Ther* 10:141–151. doi:10.1038/sj.cgt.7700546
- Liu Z, Kiessling F, Gatjens J (2010) Advanced nanomaterials in multimodal imaging: design, functionalization, and biomedical applications. *Journal of Nanomaterials* 2010:894303. doi:10.1155/2010/894303
- Maxwell DJ, Taylor JR, Nie S (2002) Self-assembled nanoparticle probes for recognition and detection of biomolecules. *Am Chem Soc* 124(32):9606–9612. doi:10.1021/ja025814p
- Nie Z, Liu KJ, Zhong C, Wang L, Yang Y, Tian Q, Liu Y (2007) Enhanced radical scavenging activity by antioxidant-functionalized gold nanoparticles: a novel inspiration for development of new artificial antioxidants. *Free Radic Biol Med* 43:1243–1254. pmid:17893037
- Orendorff CJ, Sau TK, Murphy C (2006) Shape-dependent plasmon-resonant gold nanoparticles. *Small* 2(5):636–639. doi:10.1002/sml.200500299
- Parveen S, Sahoo SK (2010) Evaluation of cytotoxicity and mechanism of apoptosis of doxorubicin using folate-decorated chitosan nanoparticles for targeted delivery to retinoblastoma. *Cancer Nanotechnology*. doi:10.1007/s12645-010-0006-0
- Raghunandan D, Basavaraja S, Mahesh B, Balaji S, Manjunath SY, Venkataraman A (2009) Biosynthesis of stable polyshaped gold nanoparticles from microwave-exposed aqueous extracellular anti-malignant guava (*Psidium guajava*) leaf extract. *Nano-Biotechnology* 5(1–4):34–41. doi:10.1007/s12030-009-9030-8
- Raghunandan D, Mahesh BD, Basavaraja S, Balaji SD, Manjunath SY, Venkataraman A (2010a) Microwave-assisted rapid extracellular synthesis of stable bio-functionalized silver nanoparticles from guava (*Psidium guajava*) leaf extract. *Journal of Nanoparticle Research*. doi:10.1007/s11051-010-9956-8
- Raghunandan D, Basavaraja S, Mahesh B, Balaji S, Manjunath SY, Venkataraman A (2010b) Rapid biosynthesis of irregular shaped gold nanoparticles from macerated aqueous extracellular dried clove buds (*Syzygium aromaticum*) solution. *Colloids and Surfaces B: Biointerfaces* 79:235–240. doi:10.1016/j.colsurfb.2010.04.003
- Rinaldo P, Matteo G, Maila S (2006) Nanosystems. Inorganic and bio-inorganic chemistry. In: Bertini I (ed) *Encyclopedia of Life Support Systems (EOLSS)*, developed under the auspices of the UNESCO. Eolss Publishers, Oxford, UK
- Sacconi S, Simkin D, Arrighi N, Chapon F, Larroque MM, Vicart S, Sternberg D, Fontaine B, Barhanin J, Desnuelle C, Bendahhou S (2009) Mechanisms underlying Andersen's syndrome pathology in skeletal muscle are revealed in human myotubes. *Am J Physiol Cell Physiol* 297:C876–C885. doi:10.1152/ajpcell.00519.2008
- Sakamoto JH et al (2010) Enabling individualized therapy through nanotechnology. *Pharmacol Res* 62(2):57–89. doi:10.1016/j.phrs.2009.12.011
- Salmaso S, Bersani S, Scomparin A, Mastrotto F, Caliceti P (2010) Supramolecular bioconjugates for protein and small drug delivery. *Isr J Chem* 50(2):160–174. doi:10.1002/ijch.201000022
- Salucci M, Stivala LA, Maiani G, Bugianesi R, Vannini V (2002) Flavonoids uptake and their effect on cell cycle of human colon adenocarcinoma cells (Caco2). *Br J Canc* 86:1645–1651. doi:10.1038/sj.bjc.6600295
- Seigneuric R, Markey L, Nuyten DSA, Dubernet C, Evelo CTA, Finot E, Garrido C (2010) From nanotechnology to nanomedicine: applications to cancer research. *Curr Mol Med* 10:640–652. doi:10.2174/156652410792630634
- Smith RA, Cokkinides V, Brooks D, Saslow D, Brawley OW (2011) Cancer screening in the United States, 2011: a review of current American Cancer Society guidelines and issues in cancer screening. *CA Cancer J Clin* 60:99–119. doi:10.3322/caac.20096
- Sperling RA, Gil PR, Zhang F, Zanella M, Parak WJ (2008) Biological applications of gold nanoparticles. *Chem Soc Rev* 37:189–1908. doi:10.1039/B712170A
- Suriamoorthy P, Zhang X, Hao G, Joly AG, Singh S, Hossu M, Sun X, Chen W (2010) Folic acid-CdTe quantum dot conjugates and their applications for cancer cell targeting. *Cancer Nanotechnology*. doi:10.1007/s12645-010-0003-3